

Attention-based Point Cloud Edge Sampling

Chengzhi Wu Junwei Zheng

Institute for Anthropomatics and Robotics,
Karlsruhe Institute of Technology, Germany

chengzhi.wu@kit.edu junwei.zheng@student.kit.edu

Julius Pfrommer Jürgen Beyerer

Fraunhofer Institute of Optronics, System Technologies
and Image Exploitation IOSB, Germany

{julius.pfrommer, juergen.beyerer}@iosb.fraunhofer.de

Abstract

Point cloud sampling is a less explored research topic for this data representation. The most common sampling methods nowadays are still classical random sampling and farthest point sampling. With the development of neural networks, various methods have been proposed to sample point clouds in a task-based learning manner. However, these methods are mostly generative-based, other than selecting points directly with mathematical statistics. Inspired by the Canny edge detection algorithm for images and with the help of the attention mechanism, this paper proposes a non-generative Attention-based Point cloud Edge Sampling method (APES), which can capture the outline of input point clouds. Experimental results show that better performances are achieved with our sampling method due to the important outline information it learned.

1. Introduction

Point cloud data is a widely used data representation in various domains including autonomous driving, augmented reality, and robotics. Due to its large-scale property in many applications, the simplification of point clouds is a fundamental and important work for 3D computer vision.

Apart from random sampling (RS), some other classical point sampling methods including grid sampling, uniform sampling, and geometric sampling have been well-established. Grid sampling samples points with regular grids and thus cannot control the number of sampled points exactly. Uniform sampling takes the points in the point cloud evenly and is more popular due to its robustness. Farthest point sampling (FPS) [9, 29] is the most representative one of them and has been widely used in lots of current methods when downsampling operations are required [19, 34, 49, 54, 58]. A more recent geometric sampling method of inverse density importance sampling (IDIS) is proposed in [11], which samples points whose distance sum values with neighbors are smaller. But this method requires the key parts of the raw point cloud have higher densities, which often is not the case. It performs even worse when the raw point cloud has an uneven distribution.

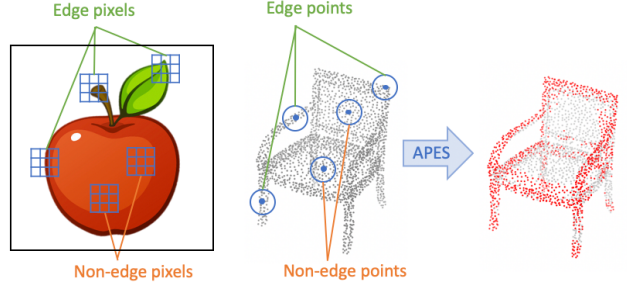


Figure 1. Similar to the Canny edge detection algorithm that detects edge pixels in images, our proposed APES algorithm samples edge points which indicate the outline of the input point clouds. The blue grids/spheres represent the local patches for given center pixels/points.

Apart from the above mathematical statistics-based methods, with the development of deep learning techniques, several neural network-based methods have been proposed for task-oriented sampling, including S-Net [8], SampleNet [16], DA-Net [21], etc. They use simple MLP to generate new sparser point clouds of desired sizes directly, supplemented with different post-processing operations. Another work of MOPS-Net [37] learns a sampling transformation matrix first, then generates the sampled point cloud by multiplying it with the original point cloud. However, all these methods are generative-based, other than selecting points directly. On the other hand, there is an increasing number of works designing neural network-based local feature aggregation operators for point clouds. Although some of them (e.g., PointCNN [19], PointASNL [54], GSS [55]) decrease the point number while learning latent features, they can hardly be considered as actual sampling methods strictly since no real spatial points exist during the processing. Moreover, none of the above methods consider shape outlines as special features.

In this paper, we propose a point cloud edge sampling method that combines neural network-based learning and mathematical statistics-based direct point selecting. One key to the success of 2D neural networks is that they can detect primary edges and use them to form shape contours implicitly in the latent space [57]. Inspired by that, we

have an assumption of using the outline points to represent the input point clouds when sampling them can be good for downstream tasks. Broadly speaking, edge detection may be considered as a special sampling strategy. Hence, by revisiting the Canny edge detection algorithm [4] which is a widely-recognized classical edge detection method for images, we propose our attention-based point cloud edge sampling (APES) method for point clouds. It uses the attention mechanism [43] to compute correlation maps and sample edge points whose properties are reflected in these correlation maps. The attention mechanism has been proven to be effective even for point cloud data [10, 12, 61]. We propose two kinds of APES with two different attention modes. Based on neighbor-to-point (N2P) attention which computes correlation maps between each point and its neighbors, local-based APES is proposed. Based on point-to-point (P2P) attention which computes a correlation map between all points, global-based APES is proposed. Our proposed method selects sampled points directly, the intermediate result preserves the point index meaning and thus can be visualized easily. Moreover, our method can sample the input point cloud to any desired size of point number.

We conclude our contributions as follows:

- A point cloud edge sampling method termed APES that combines neural network-based learning and mathematical statistics-based direct point selecting.
- Two variants of local-based APES and global-based APES, by using two different attention modes.
- Good qualitative and quantitative results on various tasks, demonstrating the effectiveness of the proposed sampling method.

2. Related Work

2.1. Point Cloud Sampling

In the past decades, non-learning-based sampling methods are mostly used for point cloud sampling. FPS [9, 29] is the most widely used sampling method, which selects the farthest points iteratively. FPS is easy to implement and has been frequently used in neural networks that aggregate local features, *e.g.*, PointNet++ [34], PointCNN [19], PointConv [49], and RS-CNN [24]. Besides, RS has also been adopted to process large-scale point clouds with great computational efficiency in lots of works, including VoxelNet [62], RandLA-Net [13] and P2B [36]. A more recently proposed method of IDIS [11] defines the inverse density importance of a point by simply adding up all distances between the center point and its neighbors, and samples points whose sum values are smaller.

Recently, learning-based sampling methods show better performances on point cloud sampling when trained in a task-oriented manner. The pioneering work of S-Net [8] generates new point coordinates directly from the

global representation. Its subsequent work of SampleNet [16] further introduces a soft projection operation for better point approximation in the post-processing step. Alternatively, DA-Net [21] extends S-Net with a density-adaptive sampling strategy, which decreases the influence of noisy points. By learning a sampling transformation matrix, MOPS-Net [37] multiplies it with the original point cloud to generate a new one as the sampled point cloud. CPL [31] samples points by investigating the output in the max-pooling layer. Replacing the MLP layers in S-Net with several self-attention layers, PST-NET [44] reports better performances on trained tasks. Its subsequent work of LighTN [45] proposes a lightweight Transformer framework for resource-limited cases.

2.2. Deep Learning on Point Clouds

Before the appearance of PointNet [33], deep learning-based methods for point cloud segmentation are usually multi-view based [1, 3, 17, 41] or volumetric-based [14, 18, 28]. PointNet [33] is the first DL-based method that learns directly on points. It uses point-wise MLP to extract global features. Its subsequent work of PointNet++ [35] further considers local information. Convolution-based methods [19, 22, 42, 48, 49, 51, 60] bring the convolution operation into point cloud feature learning. For example, PointConv [49] and KPConv [42] propose point-wise convolution operators with which points are convoluted with neighbor points. Graph-based methods [5, 20, 23, 24, 46, 52, 59] analyze point clouds by using graph structure. For example, Simonovsky *et al.* [39] take each point as a graph vertex and apply graph convolution. In DGCNN [46], EdgeConv blocks update the neighbor information dynamically based on dynamic graphs. More recently, Attention-based methods [2, 7, 10, 12, 13, 26, 27, 32] are starting to trend. PCT [12] pioneers in this direction by replacing the encoder layers in the PointNet framework with self-attention layers, while PT [61] is based on U-Net [38]. 3DCTN [27] uses off-set attention blocks, while a deformable self-attention module is proposed in SA-Det3D [2], and a dual self-attention module is proposed in 3DPCT [26]. PatchFormer [7] employs a lightweight patch-based attention block. Stratified Transformer [15] is proposed to additionally sample distant points as keys to capture long-range contexts.

3. Methodology

3.1. Revisiting Canny Edge Detection on Images

The Canny edge detector is an edge detection operator that uses a multi-stage algorithm to detect a wide range of edges in images. It consists of five steps: (i) Apply Gaussian filter to smooth the image; (ii) Find the intensity gradients of the image; (iii) Apply gradient magnitude thresholding or lower bound cut-off suppression; (iv) Apply double thresh-

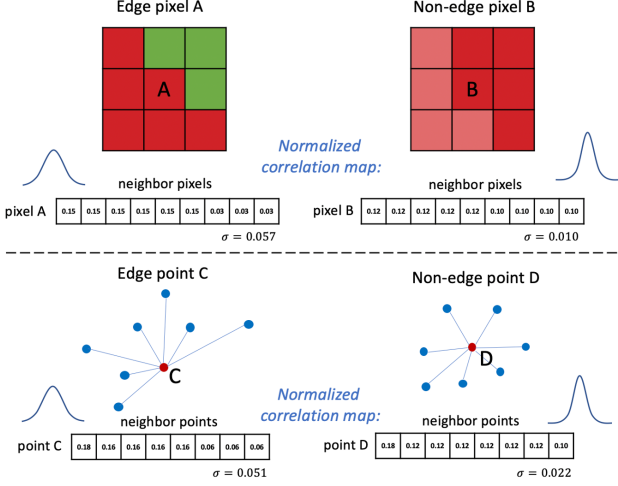


Figure 2. Illustration of using standard deviation to select edge pixels/points. The center pixel/point is self-contained as a neighbor. A larger standard deviation in the normalized correlation map means a higher possibility that it is an edge pixel/point.

old to determine potential edges; (v) Finalize the detection of edges by suppressing all the other edges that are weak and not connected to strong edges.

The key to the effectiveness of the Canny edge detection algorithm is how the edge pixels are defined. The intensity gradient of each pixel is computed with its neighbor pixels, which are usually pixels within a 3×3 or 5×5 patch. A pixel with larger changes in its patch pixel intensities indicates that its intensity gradient is larger, hence it is defined as an edge pixel. We can also interpret it in another way. **Considering each patch as a set of pixels S_p , if there are larger changes in the patch pixel intensities, the intensities of pixels in set S_p have a larger standard deviation.** Hence, an alternative method for image edge detection is to define the pixels whose patch sets have larger standard deviations as potential edge pixels, and then select them with a pre-defined threshold or get a certain number of pixels of the largest deviation values by sorting.

We further introduce a patch-wise normalized version by using neighbor correlation other than intensity. With a metric $h(p_i, p_{ij})$ defined as the correlation between the center pixel p_i and one neighbor pixel $p_{ij} \in S_p$ (larger correlation means more similar pixel features), a normalized correlation map between the center pixel and all neighbors can be computed with $h(\cdot)$ and a *softmax* operation. For one non-edge pixel, its neighbors mostly have similar features thus the standard deviation of the normalized correlation map is relatively small; while **for edge pixels, the standard deviation of the normalized correlation map is larger.** An illustrative demo is given in the top row of Figure 2. When the neighbor number k is fixed (e.g., $k = 9$ in the demo, the center pixel is self-contained as a neighbor), for all patches,

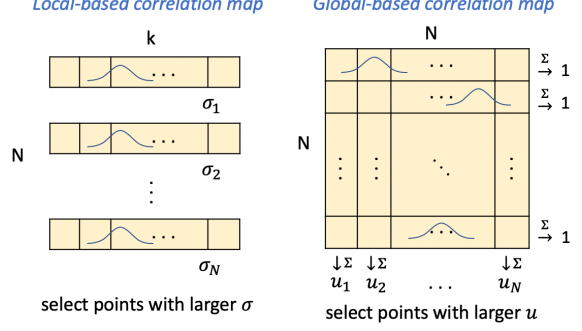


Figure 3. The key idea of proposed methods. N denotes the total number of points, while k denotes the number of neighbors used for local-based sampling method.

the mean values of their normalized correlation maps are all $1/k$. However, for edge pixels, the standard deviations of their normalized correlation maps are larger. The metric $h(\cdot)$ can be defined directly on the pixel color values, or on the pixel latent features if neural networks are used.

For images, the proposed alternative edge detection algorithm is too complex and computationally expensive compared to other widely used ones. However, it provides a possibility to transfer the idea to point clouds for point cloud edge sampling.

3.2. Local-based Point Cloud Edge Sampling

Unlike 2D images where pixels are well-aligned and patch operators can be easily defined and applied, 3D point clouds are usually irregular, unordered, and potentially sparse. Common voxel-based 3D convolution kernels are not applicable anymore in this case. Moreover, unlike each pixel that has a color value (either RGB or grey value), for many point cloud data, point coordinate is the only feature. Although it is possible to define coordinate-based point space gradients since each point cloud patch can be considered as a sub-manifold, its meaning is totally different from the meaning of pixel intensity gradients in images. It is not suitable for sampling edge points.

Here, we adapt the aforementioned patch set standard deviation-based method for point clouds. As illustrated in the bottom row of Figure 2, when the neighbor number k is fixed (e.g., $k = 8$ in the demo, the center point is self-contained as a neighbor), for all patches, the mean values of their normalized correlation maps are all $1/k$. However, for edge points, the standard deviations of their normalized correlation maps are larger.

The attention mechanism is the perfect choice for computing correlation maps between points and their neighbor sets, i.e., **the attention map is served as the normalized correlation map** directly. Same as for image pixels, for each point p_i in the input point cloud, we aggregate a local patch set S_{p_i} containing k nearest neighbor points

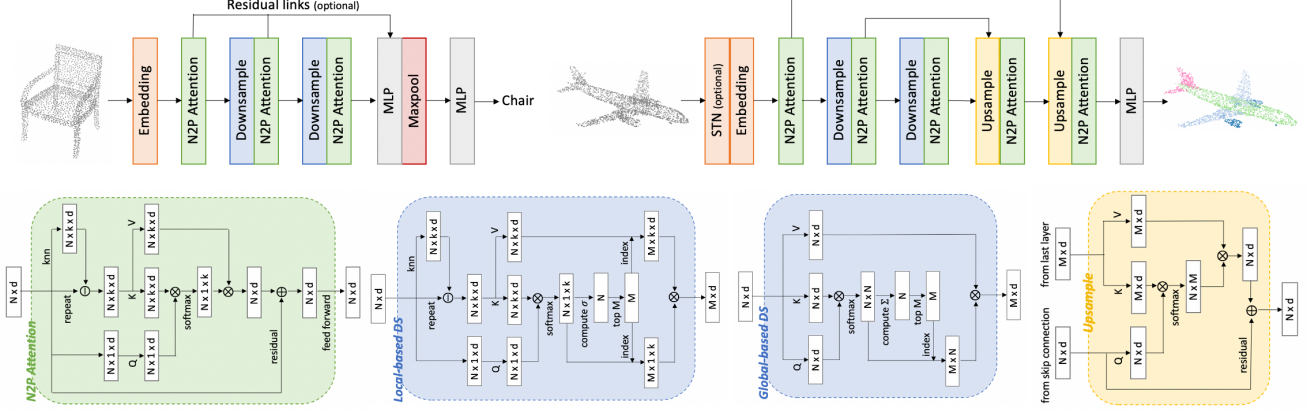


Figure 4. Network architectures for classification (top left) and segmentation (top right). The structures of N2P attention feature learning layer (bottom left), two alternative downsample layers (bottom middle), and upsample layer (bottom right) are also given. Both kinds of downsample layers downsample a point cloud from N points to M points, while upsample layer upsamples it from M points to N points.

$p_{i1}, p_{i2}, \dots, p_{ik}$. The metric $h(\cdot)$ is defined as

$$h(p_i, p_{ij}) \triangleq Q(f_{p_i}) \cdot K(f_{p_{ij}} - f_{p_i}) \quad (1)$$

where Q and K stand for the linear layers applied on the query input and the key input, respectively. Here we use the latent feature of a center point f_{p_i} as the query input, and use the latent feature difference between the neighbor point and the center point $f_{p_{ij}} - f_{p_i}$ as the key input. The feature difference $f_{p_{ij}} - f_{p_i}$ is also used as the value branch input in the later step. Note that K is shared for all neighbor points in the set \mathbf{S}_{p_i} . With a softmax layer applied by default in the attention block for normalization, the final correlation map M_{p_i} is given as

$$M_{p_i} = \text{softmax} \left(h(p_i, \mathbf{S}_{p_i}) / \sqrt{d} \right) \quad (2)$$

where $\mathbf{S}_{p_i} = \{p_{i1}, p_{i2}, \dots, p_{ik}\}$ and d is the feature dimension of the layer input. \sqrt{d} serves as a scale factor as in the original Transformer model [43].

Finally, for a point cloud of N points, correlation map standard deviations of σ_{p_i} are computed for all M_{p_i} ($i = 1, 2, \dots, N$) and sorted. Now we can simply sample the input point cloud to an edge-focused point cloud of $N/2$ points by **selecting the points whose σ_{p_i} rank in top $N/2$** .

3.3. Global-based Point Cloud Edge Sampling

We termed the above-applied attention as neighbor-to-point (N2P) attention. It focuses on capturing local information with patches. For sampling problems, global information is also crucial. Considering the special situation of using all points as the neighbor to all points (*i.e.*, $k = N$), a new global correlation map M_g of size $N \times N$ can be obtained with the linear layers Q and K being shared for all points. Now the N2P attention simplifies into the common

self-attention. We termed it point-to-point (P2P) attention in this paper. In this case, the correlation metric $h(\cdot)$ and the correlation map for each point p_i is defined as:

$$h(p_i, p_j) \triangleq Q(f_{p_i}) \cdot K(f_{p_j}) \quad (3)$$

$$M_{p_i} = \text{softmax} \left(h(p_i, \mathcal{P}) / \sqrt{d} \right) \quad (4)$$

where $\mathcal{P} = \{p_1, p_2, \dots, p_N\}$ is the input point cloud and d is the feature dimension of the layer input. The global correlation map M_g is hence determined as:

$$M_g = \begin{pmatrix} \text{---} & M_{p_1} & \text{---} \\ \text{---} & M_{p_2} & \text{---} \\ & \vdots & \\ \text{---} & M_{p_N} & \text{---} \end{pmatrix} \quad (5)$$

M_g is not a symmetric matrix and the sum of its each row is 1. Since it is an all points to all points attention and no neighbor selection process is performed, for each M_{p_i} , its correlated points are no longer reordered. All M_{p_i} has the same correlation points order which is identical to the point input order of the raw point cloud. Note that the attention result for each point is not affected by this point input order.

With the global correlation map M_g , instead of computing row-wise standard deviations for selecting points, we propose an alternative approach. Denote m_{ij} as the value of i th row and j th column in M_g . For point p_i , if it is an edge point, M_{p_i} has a larger standard deviation. In this case, considering its neighboring area, if a point p_j is more close (based on 3d spatial space or latent space) to p_i , m_{ij} is larger and p_j is also likely to be an edge point. Given this property, now consider M_g column-wise. For a point p_j , in order to make it an edge point, it needs to rank a higher value of m_{ij} in M_{p_i} more often with regard to

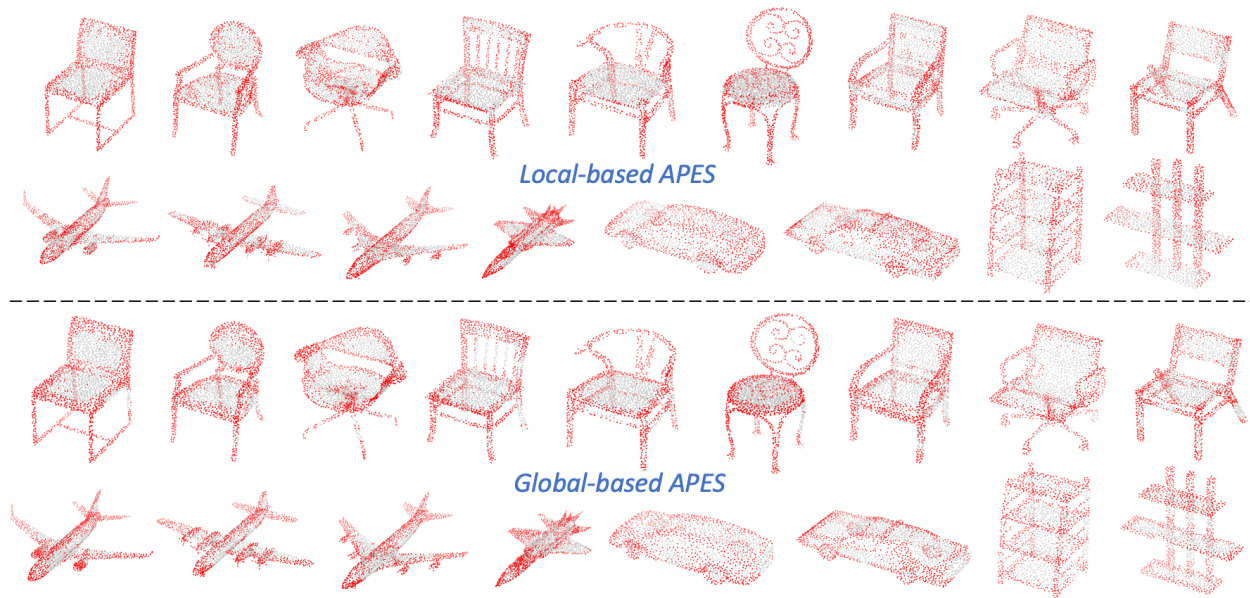


Figure 5. Visualized sampling results of local-based APES and global-based APES on different shapes. All shapes are from the test set.

other points. Hence **instead of computing row-wise standard deviations, we compute column-wise sums**. Denote $u_j = \sum_i m_{ij}$, we can simply sample the input point cloud to a point cloud of $N/2$ points by **selecting the points whose u_j rank in top $N/2$** . Overall, we can consider it as, if a point contributes more (getting a higher correlation value with regard to other points) in the self-attention correlation map, it is more likely to be a key point of the raw point cloud. An illustrative figure of those proposed two methods is given as Figure 3.

4. Experimental Results

4.1. Classification

Dataset. ModelNet40 [50] contains 12311 manufactured 3D CAD models in 40 common object categories. For a fair comparison, we use the official train-test split, in which 9843 models are used for training and 2468 models for testing. From each model mesh surface, points are uniformly sampled and normalized to the unit sphere. Only XYZ coordinates are used as point cloud input. For data augmentation, we randomly scale, rotate, and shift each object point cloud in the 3D space. During test, no data augmentation or voting methods were used.

Network Architecture Design. The classification network architecture is given in Figure 4. The embedding layer converts the input 3-dimensional XYZ feature into a higher-dimensional feature with multiple EdgeConv blocks. For feature learning layers, it is possible to use the layers designed for a similar purpose in other papers. Alternatively, the aforementioned N2P attention or P2P attention can also

Method	Overall Accuracy
PointNet [33]	89.2%
PointNet++ [34]	91.9%
SpiderCNN [53]	92.4%
DGCNN [47]	92.9%
PointCNN [19]	92.2%
PointConv [49]	92.5%
PVCNN [25]	92.4%
KPCConv [42]	92.9%
PointASNL [54]	93.2%
PT ¹ [10]	92.8%
PT ² [61]	93.7%
PCT [12]	93.2%
PRA-Net [6]	93.7%
PAConv [51]	93.6%
CurveNet [30]	93.8%
DeltaConv [48]	93.8%
APES (local-based)	93.5%
APES (global-based)	93.8%

Table 1. Classification results on ModelNet40. In comparison with other SOTA methods that also only use raw point clouds as input. Note that our reported results did not consider the voting strategy.

be used as feature learning layers. We use $k = 32$ neighbor points as default in local-based APES downsample layers. For an input point cloud of N points from the previous layer, each downsample layer samples it to $N/2$ points. Note that our method can actually sample the point cloud to any desired number of points. The optional residual links are used for better feature transmission.

Training Details. To train the model, we use AdamW optimizer with an initial learning rate 1×10^{-4} and decay it

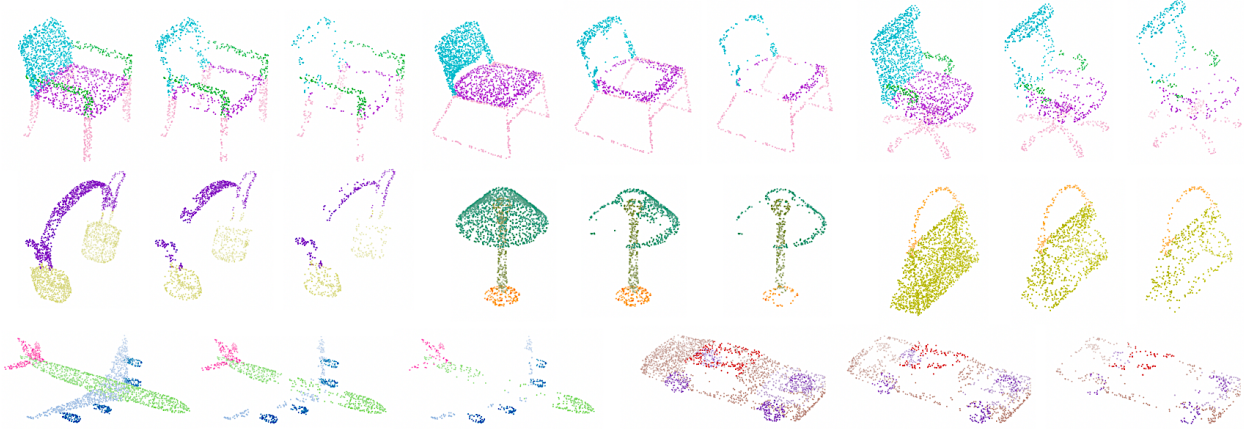


Figure 6. Visualized segmentation results as shape point clouds are downsampled. All shapes are from the test set.

to 1×10^{-8} with a cosine annealing schedule. The weight decay hyperparameter for network weights is set as 1. The dropout with a probability of 0.5 is used in the last two fully connected layers. We train the network with a batch size of 8 for 200 epochs.

Quantitative and Qualitative Results. The quantitative comparison with the SOTA methods is summarized in Table 1, where our proposed APES is among the best-performing methods. Qualitative results are presented in Figure 5. From it, we can observe that both local-based APES and global-based APES achieve good edge sampling results. On the other hand, local-based APES focuses more strictly on edge points, while global-based APES leverages a bit more on other non-edge points that are close to the edges. For example, in chair shapes, global-based APES discards some chair leg points and selects more points for chair seat edges to make the edges “thicker”. We contribute its slightly better quantitative results to this. Moreover, in our classification neural network, the training loss is simply task-oriented. Local-based APES always imposes stronger mathematical statistics constraints during the loss minimization, while global-based APES pursues better performance on the loss by allowing sampling the points that are less belong to the edge yet more useful globally.

4.2. Part Segmentation

Dataset. The ShapeNetPart dataset [56] is annotated for 3D object part segmentation. It consists of 16,880 models from 16 shape categories, with 14,006 3D models for training and 2,874 for testing. The number of parts for each category is between 2 and 6, with 50 different parts in total. We use the sampled point sets produced in [34] for a fair comparison with prior work. For evaluation metrics, we report category mIoU and instance mIoU.

Network Architecture Design. The segmentation network architecture is given in Figure 4. Most network layers

Method	Cat. mIoU	Ins. mIoU
PointNet [33]	80.4%	83.7%
PointNet++ [34]	81.9%	85.1%
SpiderCNN [53]	82.4%	85.3%
DGCNN [47]	82.3%	85.2%
SPLATNet [40]	83.7%	85.4%
PointCNN [19]	84.6%	86.1%
PointConv [49]	82.8%	85.7%
KPCConv [42]	85.0%	86.2%
PT ¹ [10]	-	85.9%
PT ² [61]	83.7%	86.6%
PCT [12]	-	86.4%
PRA-Net [6]	83.7%	86.3%
PAConv [51]	84.6%	86.1%
CurveNet [30]	-	86.6%
StratifiedTransformer [15]	85.1%	86.6%
APES (local-based)	83.1%	85.6%
APES (global-based)	83.7%	85.8%

Table 2. Segmentation results on ShapeNet Part.

Method	Points			Cat. mIoU (%)			Ins. mIoU (%)		
	2048	1024	512	2048	1024	512	2048	1024	512
APES (local)	83.11	85.56	86.17	85.58	87.27	87.41			
APES (global)	83.67	84.86	85.44	85.81	87.78	88.06			

Table 3. Segmentation results of the full point clouds and intermediate downsampled point clouds of different sizes.

are identical to the layers in the classification model, except for the spatial transform network (STN) and the upsample layer. The optional STN layer learns a spatial transformation matrix to transform the input cloud for better initial alignment. The upsample layer is a cross attention-based layer to map the input point cloud to an upsampled size. Its key and value input is the feature from the last layer, while the query input is the corresponding residual feature within the downsample process.

Method	Feature Learning Layer	OA (%)
DGCNN	EdgeConv	92.90
APES (local-based)	EdgeConv	93.02
	P2P Attention	93.30
	N2P Attention	93.47
APES (global-based)	EdgeConv	93.18
	P2P Attention	93.46
	N2P Attention	93.81

Table 4. Ablation study of using different feature learning layers in the classification network.

Training Details. To train the model, we use AdamW optimizer with an initial learning rate 1×10^{-4} and decay it to 1×10^{-8} with a cosine annealing schedule. The weight decay hyperparameter for network weights is set as 1×10^{-4} . The dropout with a probability of 0.5 is used in the last two fully connected layers. We train the network with a batch size of 16 for 200 epochs.

Quantitative and Qualitative Results. The segmentation quantitative results are given in Table 2. Our method achieves decent performance but is still far from the best ones. However, as we compute the same metrics on the intermediate downsampled point clouds in Table 3, we surprisingly find that their performances are extremely good, even far better than the SOTA methods. This indicates the downsampled edge points contribute more to the performance, while the features of the discarded non-edge points are not well reconstructed by the upsample layer. Most other neural network papers use FPS for downsampling and FPS preserves a similar data distribution compared to the original point cloud. When upsampling, simple interpolation operations [15, 34, 61] are used to create new points. However, our method focuses on edge points and the sampled result has a quite different data distribution than the original point cloud. For non-edge points, especially those far from edges, neighbor-based interpolation methods are no longer applicable. We have designed a cross attention-based layer for upsampling, but it is still very hard to get the features of the former discarded points back, even with residual links. Note that in this case, the upsampling problem actually turns into a point cloud completion or reconstruction task, which is another advanced topic for point cloud analysis. We would like to leave this for future work. The qualitative segmentation results are given in Figure 6, intermediate visualization results are also provided.

4.3. Ablation study

In this subsection, multiple ablation studies are conducted regarding the design choices of neural network architectures. All following experiments are performed on the classification benchmark of ModelNet40.

Feature Learning Layer The feature learning layer we

Method	Embedding Dimension	OA (%)
APES (local-based)	64	93.10
	128	93.47
	192	93.54
APES (global-based)	64	93.34
	128	93.81
	192	93.83

Table 5. Ablation study of using different number of embedding dimensions for the classification task.

k	8	16	32	64	128	256	512
OA (%)	93.14	93.26	93.47	93.52	93.54	93.59	93.63

Table 6. Ablation study of using different number of neighbors for local-based edge sampling.

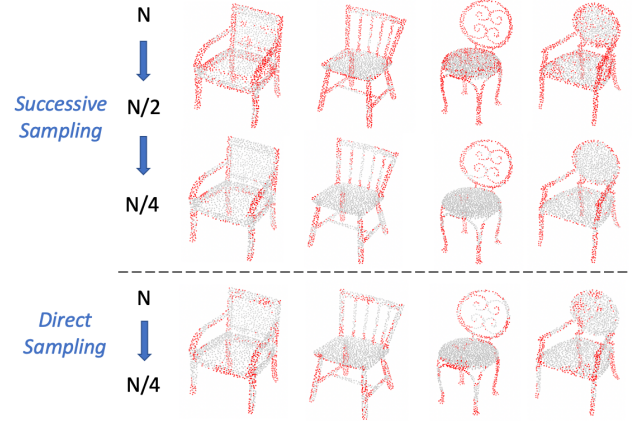


Figure 7. Sampling results of successively sampling the raw point cloud to quarter and directly sampling it to quarter.

used in the above experiments is the N2P attention layer. However, as discussed in Section 4.1, it is possible to replace it with other feature layers. We additionally report the results of using EdgeConv or P2P attention as the feature learning layer in Table 4. From it, we can observe that N2P attention achieves the best performance. Meanwhile, the results of using EdgeConv are improved when using our proposed sampling methods.

Embedding Dimension In most network-based methods, it is often reported that better performances are achieved when a larger embedding dimension is used. In our experiments, we use an embedding dimension of 128 as the default. We additionally report the results of using embedding dimensions of 64 and 192 in Table 5.

Choice of k in local-based APES When local-based APES is used, the parameter of neighbor number k is a very important parameter since it decides the perception area size of local patches. We additionally report the results of using different k in Table 6.

N_{ds}	Voxel	RS	FPS [9]	S-NET [8]	PST-NET [44]	SampleNet [16]	MOPS-Net [37]	DA-Net [21]	LighTN [45]	APES (local)	APES (global)
512	73.82	87.52	88.34	87.80	87.94	88.16	86.67	89.01	89.91	90.79	90.81
256	73.50	77.09	83.64	82.38	83.15	84.27	86.63	86.24	88.21	90.38	90.40
128	68.15	56.44	70.34	77.53	80.11	80.75	86.06	85.67	86.26	89.73	89.77
64	58.31	31.69	46.42	70.45	76.06	79.86	85.25	85.55	86.51	88.68	89.57
32	20.02	16.35	26.58	60.70	63.92	77.31	84.28	85.11	86.18	86.49	88.56

Table 7. Comparison with other sampling methods. Evaluated on the ModelNet40 classification benchmark with multiple sampling sizes.

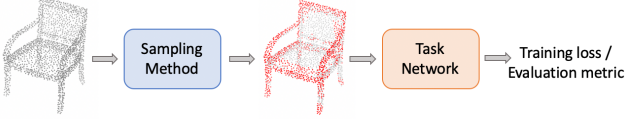


Figure 8. Framework for sampling methods evaluation.

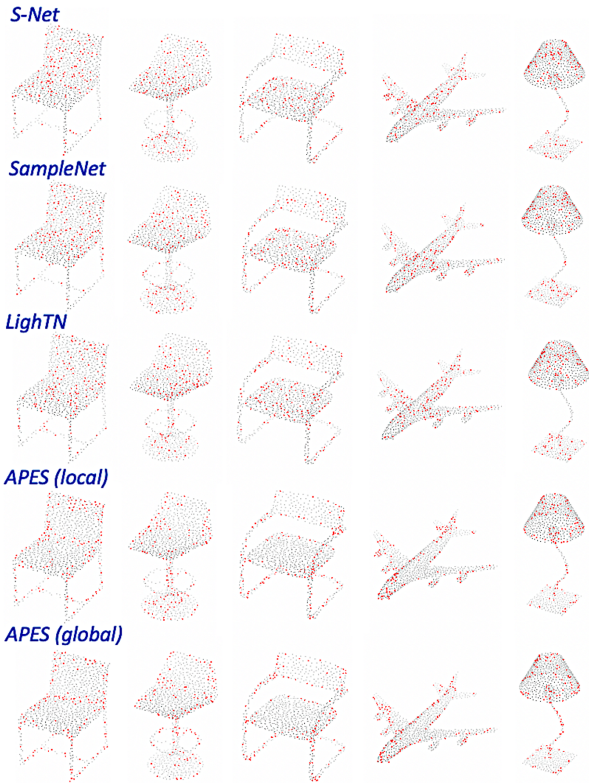


Figure 9. Visualization results of sampling 128 points from input point clouds of 1024 points with various methods. The sampling ratio is 8. Bested viewed with zoom-in.

Successive sampling vs. Direct sampling An advantage of our proposed method is that we can sample any desired number of points with it. We further provide qualitative comparison results of successively sampling the raw point cloud to quarter ($N \rightarrow N/2 \rightarrow N/4$) and directly sampling it to quarter ($N \rightarrow N/4$) in Figure 7. From it, we can observe that the sampled results are similar in most cases, while in some certain cases where exist strong edge points, successive sampling captures them better.

5. Sampling Methods Comparison

5.1. Experiment Setting

We additionally compare our sampling method with former reviewed other ones, including RS, FPS, and more recent learning-based S-Net, SampleNet, LighTN, etc. We use a same evaluation framework used in [8, 16, 45], as illustrated in Figure 8. The task here is the ModelNet40 Classification, and the task network is PointNet. Sampling methods are evaluated with multiple sampling sizes.

As discussed in the results part of Section 4.2, edge points-based sampling makes the sampled result has a quite different data distribution compared to the original point cloud, especially when a large sample ratio (defined as N_o/N_{ds}) is used. Hence for a fair comparison, we sample the input cloud to a size of $2N_{ds}$ with FPS first, then sample it to the desired size N_{ds} with proposed APES.

5.2. Quantitative and Qualitative Results

Quantitative results are given in Table 7, from which we can observe that both local-based and global-based APES achieve good classification results with the task network, under different sampling ratios. Additional qualitative results are provided in Figure 9. Although other learning-based methods achieve good numerical results, it is hard to recognize their sampling patterns from the visualized results. Their results look quite similar to random sampling. On the other hand, our proposed method shows a comprehensive sampling pattern of sampling point cloud outlines.

6. Conclusion

In this paper, an attention-based point cloud edge sampling (APES) method is proposed. It uses the attention mechanism to compute correlation maps and sample edge points accordingly. Both local-based APES and global-based APES are proposed based on two different attention modes. Qualitative and quantitative results show that our method achieves excellent performance on various tasks.

For future work, since only a simple task-oriented loss is used in our method currently, it is possible to define other supplementary losses for the training. Moreover, as we noticed the current upsampling operation hinders the segmentation performance, it would also be interesting to design a better upsampling method.

References

- [1] Nicolas Audebert, Bertrand Le Saux, and Sébastien Lefèvre. Semantic segmentation of earth observation data using multimodal and multi-scale deep networks. In *Asian conference on computer vision*, pages 180–196. Springer, 2016. 2
- [2] Prarthana Bhattacharyya, Chengjie Huang, and K. Czarnecki. Sa-det3d: Self-attention based context-aware 3d object detection. *2021 IEEE/CVF International Conference on Computer Vision Workshops (ICCVW)*, pages 3022–3031, 2021. 2
- [3] Alexandre Boulch, Bertrand Le Saux, and Nicolas Audebert. Unstructured point cloud semantic labeling using deep segmentation networks. *3DOR@ Eurographics*, 3, 2017. 2
- [4] John F. Canny. A computational approach to edge detection. *IEEE Transactions on Pattern Analysis and Machine Intelligence*, PAMI-8:679–698, 1986. 2
- [5] Can Chen, Luca Zanotti Fragonara, and Antonios Tsourdos. Gapnet: Graph attention based point neural network for exploiting local feature of point cloud. *Neurocomputing*, 438:122–132, 2021. 2
- [6] Silin Cheng, Xiwu Chen, Xinwei He, Zhe Liu, and Xiang Bai. Pra-net: Point relation-aware network for 3d point cloud analysis. *IEEE Transactions on Image Processing*, 30:4436–4448, 2021. 5, 6
- [7] Zhang Cheng, Haocheng Wan, Xinyi Shen, and Zizhao Wu. Patchformer: A versatile 3d transformer based on patch attention. *ArXiv*, abs/2111.00207, 2021. 2
- [8] Oren Dovrat, Itai Lang, and Shai Avidan. Learning to sample. *2019 IEEE/CVF Conference on Computer Vision and Pattern Recognition (CVPR)*, pages 2755–2764, 2019. 1, 2, 8
- [9] Yuval Eldar, Michael Lindenbaum, Moshe Porat, and Yehoshua Y. Zeevi. The farthest point strategy for progressive image sampling. *Proceedings of the 12th IAPR International Conference on Pattern Recognition, Vol. 2 - Conference B: Computer Vision & Image Processing. (Cat. No.94CH3440-5)*, pages 93–97 vol.3, 1994. 1, 2, 8
- [10] Nico Engel, Vasileios Belagiannis, and Klaus C. J. Dietmayer. Point transformer. *IEEE Access*, 9:134826–134840, 2021. 2, 5, 6
- [11] Fabian Groh, Patrick Wieschollek, and Hendrik P. A. Lensch. Flex-convolution - million-scale point-cloud learning beyond grid-worlds. In *ACCV*, 2018. 1, 2
- [12] Meng-Hao Guo, Junxiong Cai, Zheng-Ning Liu, Tai-Jiang Mu, Ralph Robert Martin, and Shimin Hu. Pct: Point cloud transformer. *Comput. Vis. Media*, 7:187–199, 2021. 2, 5, 6
- [13] Qingyong Hu, Bo Yang, Linhai Xie, Stefano Rosa, Yulan Guo, Zhihua Wang, Agathoniki Trigoni, and A. Markham. Randla-net: Efficient semantic segmentation of large-scale point clouds. *2020 IEEE/CVF Conference on Computer Vision and Pattern Recognition (CVPR)*, pages 11105–11114, 2020. 2
- [14] Mingyang Jiang, Yiran Wu, Tianqi Zhao, Zelin Zhao, and Cewu Lu. Pointsift: A sift-like network module for 3d point cloud semantic segmentation. *arXiv preprint arXiv:1807.00652*, 2018. 2
- [15] Xin Lai, Jianhui Liu, Li Jiang, Liwei Wang, Hengshuang Zhao, Shu Liu, Xiaojuan Qi, and Jiaya Jia. Stratified transformer for 3d point cloud segmentation. *2022 IEEE/CVF Conference on Computer Vision and Pattern Recognition (CVPR)*, pages 8490–8499, 2022. 2, 6, 7
- [16] Itai Lang, Asaf Manor, and Shai Avidan. Samplenet: Differentiable point cloud sampling. *2020 IEEE/CVF Conference on Computer Vision and Pattern Recognition (CVPR)*, pages 7575–7585, 2020. 1, 2, 8
- [17] Felix Järemo Lawin, Martin Danelljan, Patrik Tosteberg, Goutam Bhat, Fahad Shahbaz Khan, and Michael Felsberg. Deep projective 3d semantic segmentation. In *International Conference on Computer Analysis of Images and Patterns*, pages 95–107. Springer, 2017. 2
- [18] Truc Le and Ye Duan. Pointgrid: A deep network for 3d shape understanding. In *Proceedings of the IEEE conference on computer vision and pattern recognition*, pages 9204–9214, 2018. 2
- [19] Yangyan Li, Rui Bu, Mingchao Sun, Wei Wu, Xinhan Di, and Baoquan Chen. Pointcnn: Convolution on x-transformed points. In *NeurIPS*, 2018. 1, 2, 5, 6
- [20] Zhidong Liang, Ming Yang, Hao Li, and Chunxiang Wang. 3d instance embedding learning with a structure-aware loss function for point cloud segmentation. *IEEE Robotics and Automation Letters*, 5:4915–4922, 2020. 2
- [21] Yanan Lin, Yan Huang, Shihao Zhou, Mengxi Jiang, Tianlong Wang, and Yunqi Lei. Da-net: Density-adaptive down-sampling network for point cloud classification via end-to-end learning. *2021 4th International Conference on Pattern Recognition and Artificial Intelligence (PRAI)*, pages 13–18, 2021. 1, 2, 8
- [22] Yiqun Lin, Zizheng Yan, Haibin Huang, Dong Du, Ligang Liu, Shuguang Cui, and Xiaoguang Han. Fpconv: Learning local flattening for point convolution. In *Proceedings of the IEEE/CVF Conference on Computer Vision and Pattern Recognition*, pages 4293–4302, 2020. 2
- [23] Zhi-Hao Lin, Sheng-Yu Huang, and Yu-Chiang Frank Wang. Convolution in the cloud: Learning deformable kernels in 3d graph convolution networks for point cloud analysis. In *Proceedings of the IEEE/CVF conference on computer vision and pattern recognition*, pages 1800–1809, 2020. 2
- [24] Yongcheng Liu, Bin Fan, Shiming Xiang, and Chunhong Pan. Relation-shape convolutional neural network for point cloud analysis. *2019 IEEE/CVF Conference on Computer Vision and Pattern Recognition (CVPR)*, pages 8887–8896, 2019. 2
- [25] Zhijian Liu, Haotian Tang, Yujun Lin, and Song Han. Point-voxel cnn for efficient 3d deep learning. *ArXiv*, abs/1907.03739, 2019. 5
- [26] Dening Lu, Kyle Gao, Qian Xie, Linlin Xu, and Jonathan Li. 3dpct: 3d point cloud transformer with dual self-attention. *ArXiv*, abs/2209.11255, 2022. 2
- [27] Dening Lu, Qian Xie, Linlin Xu, and Jonathan Li. 3dctn: 3d convolution-transformer network for point cloud classification. *ArXiv*, abs/2203.00828, 2022. 2
- [28] Daniel Maturana and Sebastian Scherer. Voxnet: A 3d convolutional neural network for real-time object recognition.

- In *2015 IEEE/RSJ International Conference on Intelligent Robots and Systems (IROS)*, pages 922–928. IEEE, 2015. 2
- [29] Carsten Moenning and Neil A. Dodgson. Fast marching farthest point sampling. In *Eurographics*, 2003. 1, 2
- [30] A. A. M. Muzahid, Wanggen Wan, Ferdous Sohel, Lianyao Wu, and Li Hou. Curvenet: Curvature-based multitask learning deep networks for 3d object recognition. *IEEE/CAA Journal of Automatica Sinica*, 8:1177–1187, 2021. 5, 6
- [31] Ehsan Nezhadarya, Ehsan Moeen Taghavi, Bingbing Liu, and Jun Luo. Adaptive hierarchical down-sampling for point cloud classification. *2020 IEEE/CVF Conference on Computer Vision and Pattern Recognition (CVPR)*, pages 12953–12961, 2020. 2
- [32] Xuran Pan, Zhuofan Xia, Shiji Song, Li Erran Li, and Gao Huang. 3d object detection with pointformer. *2021 IEEE/CVF Conference on Computer Vision and Pattern Recognition (CVPR)*, pages 7459–7468, 2021. 2
- [33] C. Qi, Hao Su, Kaichun Mo, and Leonidas J. Guibas. Pointnet: Deep learning on point sets for 3d classification and segmentation. *2017 IEEE Conference on Computer Vision and Pattern Recognition (CVPR)*, pages 77–85, 2017. 2, 5, 6
- [34] C. Qi, L. Yi, Hao Su, and Leonidas J. Guibas. Pointnet++: Deep hierarchical feature learning on point sets in a metric space. In *NIPS*, 2017. 1, 2, 5, 6, 7
- [35] Charles R Qi, Li Yi, Hao Su, and Leonidas J Guibas. PointNet++: Deep hierarchical feature learning on point sets in a metric space. *arXiv preprint arXiv:1706.02413*, 2017. 2
- [36] Haozhe Qi, Chen Feng, ZHIGUO CAO, Feng Zhao, and Yang Xiao. P2b: Point-to-box network for 3d object tracking in point clouds. *2020 IEEE/CVF Conference on Computer Vision and Pattern Recognition (CVPR)*, pages 6328–6337, 2020. 2
- [37] Yu Qian, Junhui Hou, Yiming Zeng, Qijian Zhang, Sam Tak Wu Kwong, and Ying He. Mops-net: A matrix optimization-driven network for task-oriented 3d point cloud downsampling. *ArXiv*, abs/2005.00383, 2020. 1, 2, 8
- [38] Olaf Ronneberger, Philipp Fischer, and Thomas Brox. U-net: Convolutional networks for biomedical image segmentation. *ArXiv*, abs/1505.04597, 2015. 2
- [39] Martin Simonovsky and Nikos Komodakis. Dynamic edge-conditioned filters in convolutional neural networks on graphs. In *Proceedings of the IEEE conference on computer vision and pattern recognition*, pages 3693–3702, 2017. 2
- [40] Hang Su, V. Jampani, Deqing Sun, Subhransu Maji, Evangelos Kalogerakis, Ming-Hsuan Yang, and Jan Kautz. Splatnet: Sparse lattice networks for point cloud processing. *2018 IEEE/CVF Conference on Computer Vision and Pattern Recognition*, pages 2530–2539, 2018. 6
- [41] Maxim Tatarchenko, Jaesik Park, Vladlen Koltun, and Qian-Yi Zhou. Tangent convolutions for dense prediction in 3d. In *Proceedings of the IEEE Conference on Computer Vision and Pattern Recognition*, pages 3887–3896, 2018. 2
- [42] Hugues Thomas, C. Qi, Jean-Emmanuel Deschaud, Beatriz Marcotequi, François Goulette, and Leonidas J. Guibas. Kpconv: Flexible and deformable convolution for point clouds. *2019 IEEE/CVF International Conference on Computer Vision (ICCV)*, pages 6410–6419, 2019. 2, 5, 6
- [43] Ashish Vaswani, Noam Shazeer, Niki Parmar, Jakob Uszkoreit, Llion Jones, Aidan N Gomez, Łukasz Kaiser, and Illia Polosukhin. Attention is all you need. *Advances in neural information processing systems*, 30, 2017. 2, 4
- [44] Xu Wang, Yi Jin, Yigang Cen, Congyan Lang, and Yidong Li. Pst-net: Point cloud sampling via point-based transformer. In *ICIG*, 2021. 2, 8
- [45] Xu Wang, Yi Jin, Yigang Cen, Tao Wang, Bowen Tang, and Yidong Li. Lightn: Light-weight transformer network for performance-overhead tradeoff in point cloud downsampling. *ArXiv*, abs/2202.06263, 2022. 2, 8
- [46] Yue Wang, Yongbin Sun, Ziwei Liu, Sanjay E Sarma, Michael M Bronstein, and Justin M Solomon. Dynamic graph cnn for learning on point clouds. *Acm Transactions On Graphics (tog)*, 38(5):1–12, 2019. 2
- [47] Yue Wang, Yongbin Sun, Ziwei Liu, Sanjay E. Sarma, Michael M. Bronstein, and Justin M. Solomon. Dynamic graph cnn for learning on point clouds. *ACM Transactions on Graphics (TOG)*, 38:1–12, 2019. 5, 6
- [48] Ruben Wiersma, Ahmad Nasikun, Elmar Eisemann, and Klaus Hildebrandt. Deltaconv: Anisotropic point cloud learning with exterior calculus. *ArXiv*, abs/2111.08799, 2021. 2, 5
- [49] Wenxuan Wu, Zhongang Qi, and Fuxin Li. Pointconv: Deep convolutional networks on 3d point clouds. *2019 IEEE/CVF Conference on Computer Vision and Pattern Recognition (CVPR)*, pages 9613–9622, 2019. 1, 2, 5, 6
- [50] Zhirong Wu, Shuran Song, Aditya Khosla, Fisher Yu, Linguang Zhang, Xiaoou Tang, and Jianxiong Xiao. 3d shapenets: A deep representation for volumetric shapes. *2015 IEEE Conference on Computer Vision and Pattern Recognition (CVPR)*, pages 1912–1920, 2015. 5
- [51] Mutian Xu, Runyu Ding, Hengshuang Zhao, and Xiaojuan Qi. Paconv: Position adaptive convolution with dynamic kernel assembling on point clouds. *2021 IEEE/CVF Conference on Computer Vision and Pattern Recognition (CVPR)*, pages 3172–3181, 2021. 2, 5, 6
- [52] Qiangeng Xu, Xudong Sun, Cho-Ying Wu, Panqu Wang, and Ulrich Neumann. Grid-gcn for fast and scalable point cloud learning. In *Proceedings of the IEEE/CVF Conference on Computer Vision and Pattern Recognition*, pages 5661–5670, 2020. 2
- [53] Yifan Xu, Tianqi Fan, Mingye Xu, Long Zeng, and Yu Qiao. Spidercnn: Deep learning on point sets with parameterized convolutional filters. *ArXiv*, abs/1803.11527, 2018. 5, 6
- [54] Xu Yan, Chaoda Zheng, Zhuguo Li, Sheng Wang, and Shuguang Cui. Pointasnl: Robust point clouds processing using nonlocal neural networks with adaptive sampling. *2020 IEEE/CVF Conference on Computer Vision and Pattern Recognition (CVPR)*, pages 5588–5597, 2020. 1, 5
- [55] Jiancheng Yang, Qiang Zhang, Bingbing Ni, Linguo Li, Jinxian Liu, Mengdie Zhou, and Qi Tian. Modeling point clouds with self-attention and gumbel subset sampling. *2019 IEEE/CVF Conference on Computer Vision and Pattern Recognition (CVPR)*, pages 3318–3327, 2019. 1
- [56] L. Yi, Vladimir G. Kim, Duygu Ceylan, I-Chao Shen, Mengyan Yan, Hao Su, Cewu Lu, Qixing Huang, Alla Sheffer, and Leonidas J. Guibas. A scalable active framework for

- region annotation in 3d shape collections. *ACM Transactions on Graphics (TOG)*, 35:1 – 12, 2016. [6](#)
- [57] Jason Yosinski, Jeff Clune, Anh M Nguyen, Thomas J. Fuchs, and Hod Lipson. Understanding neural networks through deep visualization. *ArXiv*, abs/1506.06579, 2015. [1](#)
- [58] Lequan Yu, Xianzhi Li, Chi-Wing Fu, Daniel Cohen-Or, and Pheng-Ann Heng. Pu-net: Point cloud upsampling network. *2018 IEEE/CVF Conference on Computer Vision and Pattern Recognition*, pages 2790–2799, 2018. [1](#)
- [59] Kuangen Zhang, Ming Hao, Jing Wang, Xinxing Chen, Yuquan Leng, Clarence W. de Silva, and Chenglong Fu. Linked dynamic graph cnn: Learning through point cloud by linking hierarchical features. *2021 27th International Conference on Mechatronics and Machine Vision in Practice (M2VIP)*, pages 7–12, 2021. [2](#)
- [60] Hengshuang Zhao, Li Jiang, Chi-Wing Fu, and Jiaya Jia. Pointweb: Enhancing local neighborhood features for point cloud processing. In *Proceedings of the IEEE/CVF conference on computer vision and pattern recognition*, pages 5565–5573, 2019. [2](#)
- [61] Hengshuang Zhao, Li Jiang, Jiaya Jia, Philip H. S. Torr, and Vladlen Koltun. Point transformer. *2021 IEEE/CVF International Conference on Computer Vision (ICCV)*, pages 16239–16248, 2021. [2](#), [5](#), [6](#), [7](#)
- [62] Yin Zhou and Oncel Tuzel. Voxelnet: End-to-end learning for point cloud based 3d object detection. *2018 IEEE/CVF Conference on Computer Vision and Pattern Recognition*, pages 4490–4499, 2018. [2](#)